



Published in final edited form as:

Mucosal Immunol. 2017 September ; 10(5): 1160–1168. doi:10.1038/mi.2016.127.

Intestinal helminth infection impacts the systemic distribution and function of the naïve lymphocyte pool

Irah L. King^{1,*}, Katja Mohrs², Alexandre P. Meli¹, Jeffrey Downey⁵, Paula Lanthier⁴, Fanny Tzelepis⁵, Jörg H. Fritz⁶, Alexei V. Tumanov³, Maziar Divangahi⁵, Elizabeth A. Leadbetter³, and Markus Mohrs^{2,*}

¹Department of Microbiology and Immunology, Microbiome and Disease Tolerance Centre, McGill University, Montreal, QC H3A 2B4

²Regeneron Pharmaceuticals, Inc., Tarrytown, NY 10591

³Department of Microbiology and Immunology, University of Texas School of Medicine Health Science Center at San Antonio, San Antonio TX 78229

⁴Trudeau Institute, Saranac Lake, NY 12983

⁵Department of Medicine, Department of Microbiology and Immunology, Department of Pathology, Meakins-Christies Laboratories, McGill International TB Centre, McGill University Health Centre, Montreal, QC H4A 3J1

⁶Department of Microbiology and Immunology, Department of Physiology, Complex Traits Group, McGill University, Montreal, QC H3G 0B1

INTRODUCTION

Continuous circulation of the homeostatic naïve lymphocyte population through lymph nodes (LNs) is a central tenet of immune surveillance. Cellular entry into and exit from these LNs are at equilibrium in the absence of overt infection or inflammation such that the number of lymphocytes present in a given LN remains remarkably constant during adult life¹. One possible reason that this set point evolved is to optimize the environment for lymphocyte survival as well as activation upon specific antigen encounter. Indeed, circulation through lymph nodes provides access to limited survival signals such as IL-7 that are required for cell survival². In further support of this hypothesis are studies in which naïve T cells of known specificity were transferred at carefully titrated numbers into recipient animals prior to peptide immunization³. This work demonstrated that when the

Users may view, print, copy, and download text and data-mine the content in such documents, for the purposes of academic research, subject always to the full Conditions of use:http://www.nature.com/authors/editorial_policies/license.html#terms

*corresponding authors Communicating author: Irah King, PhD, Assistant Professor, McGill University, 3775 University Street, Room 402, Montreal, QC H3A 2B4, irah.king@mcgill.ca, (514) 398-7325.

AUTHOR CONTRIBUTIONS

I.L.K. designed and performed experiments, analyzed data and wrote the manuscript. K.M., A.P.M., J.D., P.L., F.T. performed experiments and analyzed data. J.H.F. provided mice. A.V.T., E.A.L. and M.D. provided reagents and conceptual input. M.M. initiated the project, analyzed data and wrote the manuscript.

DISCLOSURE

The authors have no conflicts of interest to declare.

number of transferred cells exceeds physiological levels, the proliferative capacity of the donor cells was compromised. Thus, LN cell number must be precisely controlled to maintain immune homeostasis and maximize responsiveness upon immune challenge.

Although homeostatic control of T and B cell populations in the LNs is well-established, the impact that local lymphoid tissue inflammation may have on the systemic pool of lymphocytes is less clear. One consequence of infection or immunization-induced inflammation is transient enlargement of LNs draining the site of immune challenge. Factors contributing to LN hyperplasia include expansion of the lymphatic⁴, fibroblast reticular cell⁵ and arterial networks^{6,7} that collectively enhance leukocyte entry into the draining LN as well as proliferative effector cell expansion and retention⁸. In experiments examining the primary Th2-driven immune response to *Heligmosomoides polygrus* (*Hp*), a strictly enteric helminth parasite, we observed dramatic and sustained enlargement of the mesenteric lymph nodes (mesLN), the primary site of adaptive immune cell activation following infection. In addition to robust expansion of CD4⁺ T and B effector cells, we unexpectedly observed a significant and persistent accumulation of naïve T and B cells in the inflamed mesLN. Subsequent experiments were performed to understand 1) the relevance of naïve lymphocyte accumulation to the primary effector cell response 2) the mechanisms underlying this accumulation and 3) its impact on the systemic distribution of the naïve lymphocyte pool and response to secondary challenge.

RESULTS

Naïve lymphocytes accumulate in the Th2 reactive mesenteric lymph nodes following enteric helminth infection

Infection of mice with the enteric helminth parasite (*Hp*) results in a robust Th2 and Type 2 humoral response initiated in the mesLN^{9,10}. This response results in a striking enlargement of the mesLN by 2 weeks post-infection and a dramatic increase in mesLN weight and total lymphocyte number (hyperplasia) as well as morphological changes due to a robust humoral immune response (Figure 1A-C). *Hp*-induced mesLN hyperplasia persisted through the chronic stage of infection (i.e. 6 weeks), yet was reduced if the parasite was eliminated using anti-helminthics at 2 weeks post-infection (Figure 1C, D). Further characterization of lymphocyte subsets in the Th2 reactive mesLN over the course of infection indicated that the total number of CD4⁺ and CD8⁺ T cells significantly increased between 1 and 4 weeks post-infection with the CD19⁺ B cell pool increasing with slightly more rapid kinetics (Figure 1E). In addition to an expected increase in the number of CD44^{hi}CD62L^{lo} effector lymphocytes (Figure 1F, see supplemental Figure 1A-C for gating), we also noticed an unexpected increase in the number of CD44^{lo}CD62L^{hi} naïve phenotype lymphocytes. In fact, the majority of the T and B lymphocytes present in the inflamed mesLN expressed a naïve phenotype (Figure 1G). These results demonstrate that naïve T and B cell accumulation occur within the Th2 reactive LN following helminth infection.

The accumulation of naïve lymphocytes is driven by an increased homeostatic set-point

Th2 differentiation and IL-4 production is critical for protective immunity to *Hp* infection¹¹. IL-4 cytokine reporter (4get) mice in which GFP identifies IL-4 expressing cells are a

sensitive ex vivo readout for Th2 differentiation¹². We have previously shown that the number of IL-4/GFP⁺ effector CD4 T cells in the mesLN begins to increase within the first 5 days of *Hp* infection and continues to expand over time, reaching its peak between 2-4 weeks post-infection¹³. In contrast, naïve T cells began to accumulate in the Th2 reactive mesLN only after 7 days post-infection (Figure 1G). To determine whether this accumulation contributed to the IL-4⁺ effector T cell response, 4get mice were treated with anti-CD62L mAb between days 7 and 14 post-infection to inhibit naïve lymphocyte entry into the mesLN¹⁴. Analysis on day 14 post-infection revealed a dramatic reduction in naïve T and B cell accumulation, as measured by a GFP⁻CD44^{lo} or IgD⁺CD44^{lo} phenotype (in lieu of CD62L), respectively, in the mesLN of infected mice (Figure 2A); however, no significant defect in the number of IL-4⁺ effector CD4 T cells was observed (Figure 2B). To further determine whether the period between 1-2 weeks post-infection represented a critical phase for naïve T and B cell accumulation, some mice treated with anti-CD62L were examined 1 week after antibody treatment was terminated (i.e. day 21 post-infection). Release of the entry blockade after the second week of infection restored the number of naïve T and B cells to isotype-treated control levels. However, again we did not observe any difference in the number of IL-4⁺ effector CD4 T cells at this time point (Figure 2A, B). Collectively, these data indicated that the accumulation of naïve T cells in the reactive mesLN beginning one week after infection does not affect IL-4⁺ effector CD4 T cell response and that the reactive mesLN represents a sustained reservoir for naïve lymphocytes due to an increased homeostatic set-point.

CD4⁺ T cell activation is required for naïve B lymphocyte accumulation

A previous study using subcutaneous immunization with antigen in Th1-polarizing CFA adjuvant demonstrated that B cells were important for LN enlargement⁴. To determine whether B cells also contribute to naïve T cell accumulation in a Th2-dominant immune response, BALB/c or B cell-deficient JhD mice were infected with *Hp* and naïve T cells were enumerated in the mesLN 2 weeks later. In contrast to CFA immunization (Angeli et al., 2006), the number of naïve T cells was not decreased in the absence of B cells, but in fact increased, compared to WT controls suggesting a potential regulatory role for B lymphocytes in naïve T cell accumulation (Figure 3A). Using a model of viral infection, Iwasaki and colleagues showed that innate immune mechanisms contributed to transient LN enlargement and naïve T cell accumulation within 48 hours of immune challenge⁶. In the case of *Hp* infection, however, we did not observe naïve T lymphocyte accumulation prior to day 7 post-infection (Figure 1A) suggesting that the adaptive immune response may play a more dominant role. Using CD19⁺IgD⁺CD44^{lo} B cells as a readout for naïve lymphocyte accumulation, BALB/c, TCR α -deficient BALB/c and CD4 T cell-depleted BALB/c mice were infected with *Hp* and the number of naïve B cells was determined 2 weeks later. In contrast to B cell-deficient mice, infected animals that lack $\alpha\beta$ T cells or were depleted of CD4⁺ cells failed to accumulate naïve B cells in their draining mesLNs (Figure 3B, C). MesLN from *Hp*-infected DO11.10 mice containing a monoclonal population of CD4⁺ T cells specific for chicken ovalbumin also failed to accumulate naïve B cells (Figure 3D), indicating that not just CD4⁺ T cells per se, but activation of this population by cognate antigen was required.

Lymphotoxin- β receptor signaling is required for naïve lymphocyte accumulation

Because naïve lymphocyte accumulation required CD4⁺ T cell activation, but was not required for the increase in IL-4⁺ effector CD4 T cells after 1 week of infection, we sought to identify factors that regulated naïve T cell accumulation independent of the Th2 response. These events could not be separated in mice unable to receive IL-4 signals because both naïve T cell accumulation and, consistent with our previous studies¹⁵, the Th2 response was compromised following *Hp* infection of IL-4R α KO mice (Figure 4A,B). In addition, experiments using mice deficient in TNF α or Type I interferon receptor (IFNAR) signals, two pathways previously shown to promote LN hyperplasia^{16,17}, demonstrated that these factors were not only dispensable for naïve lymphocyte accumulation following *Hp* infection but may actually exert regulatory effects, at least on T cell accumulation (Figure 4C, D and supplemental Figure 3A, B).

Lymphotoxin β receptor (LT β R) has been previously shown to play a role in Type 2 immunity following *Hp* infection and mice deficient in the LT β R ligands experience compromised LN hyperplasia following subcutaneous immunization with CFA¹⁸⁻²⁰. However, in these studies LT β R signals were inhibited at the time of infection or immunization, potentially compromising initial dendritic cell (DC)-dependent T cell recruitment to the mesLN²¹. Since naïve T lymphocytes do not accumulate prior to establishment of a robust Th2 response (i.e. 1 week after *Hp* infection; Figure 1), we blocked LT signaling by administering LT β R-Ig on days 7 and 10 and assessed naïve T cell accumulation and the IL-4⁺ effector CD4 T cell response on day 14. Compared to control animals, naïve T and B cells failed to accumulate in the mesLN of LT β R-Ig-treated mice (Figure 4E). Importantly, the treatment resulted only in a subtle, albeit significant, reduction in the number of IL-4/GFP⁺ expressing CD4⁺ T cells (Figure 4F). These results were most likely not due to a change in lymphocyte survival as the frequency of active Caspase-3⁺ cells (a marker of apoptosis) was not different between the groups (supplemental Figure 3C-E).

A previous report described an important role for LT β production by B cells in LN hyperplasia and remodeling during *Hp* infection²⁰. While we found that LT signals were also important for naïve T cell accumulation, our results indicated that B cells were not required suggesting that other cellular sources of LT β R ligands contribute to this process. To examine whether other LN cell populations express ligands for LT β R including LT $\alpha\beta$ and LIGHT, DCs, B cells and CD4⁺ T cells were sorted from the mesLN of *Hp*-infected mice and *Lta*, *Ltb* and *Tnfsf14* (encoding for LIGHT) were measured by qRT-PCR. Although both *Lta* and *Ltb* were expressed at high levels by all immune cell subsets examined (data not shown), their relative difference compared to B cells was small (Figure 4G). By contrast, both DCs and CD4⁺ T cells expressed high levels of *Tnfsf14* mRNA compared to B cells (Figure 4G). Collectively, these data indicate that LT β R-dependent signals, possibly from multiple immune cell subsets, orchestrate the accumulation of naïve lymphocytes in the inflamed mesLN independent of its effects on initial Th2 differentiation or cell survival following helminth infection.

Loss of naïve lymphocytes from non-draining LN during *Hp* infection

The striking and persistent accumulation of naïve lymphocytes in the mesLN of *Hp*-infected animals prompted us to identify the site(s) from where these cells may derive. Although the thymus generates new naïve T lymphocytes and the spleen contains a large number of naïve T and B cells that could potentially be recruited to inflamed sites, neither thymectomy nor splenectomy of adult mice prior to infection affected the accumulation of naïve T and B cells (unpublished observations). However, the number of lymphocytes and naïve T and B cell subsets in non-draining LN (e.g. inguinal, axillary, and brachial LNs) were significantly reduced at 2 weeks after *Hp* infection compared to uninfected controls (Figure 5A). To test whether the naïve lymphocyte redistribution occurred in an antigen-independent manner, OVA-specific CD4⁺ T cells were purified from DO11.10 mice and transferred into Thy1 congenic uninfected mice or mice infected with *Hp* 11 days prior. One hour after transfer, ten-fold more donor KJ1-26⁺ DO11.10 T cells were found in the mesLN of *Hp* infected mice compared to uninfected controls (as determined by FACS; Figure 5B). Consistent with the infection-induced redistribution of the polyclonal naïve lymphocyte population from the peripheral LNs, there were significantly fewer donor DO11.10 cells in the peripheral LNs of infected mice compared to uninfected controls (Figure 5B). The full extent of the systemic redistribution was revealed by comparing the accumulation of donor T cells in the mesLN relative to the skin-draining LN in the same animal (Figure 5C). These data indicate that the systemic naïve lymphocyte pool can be redistributed in an antigen-independent manner following an enteric helminth infection.

Hp infection compromises immunity to heterologous challenge at peripheral sites

Landmark studies by Moon et al. demonstrated that the starting number of naïve lymphocytes specific for a given antigen predicts the magnitude of the primary adaptive immune response following immunization with relevant peptide²². Because helminth infection effectively decreased the naïve lymphocyte number in non-draining LNs, we reasoned that the magnitude of the immune response to heterologous challenge at peripheral sites might be compromised in helminth-infected mice. To test this hypothesis, we employed several distinct methods of heterologous challenge to measure the antigen-specific response at peripheral sites of helminth-infected mice. First, at 2 weeks post-infection with *Hp*, mice were immunized with the T-dependent antigen 4-hydroxy-3-nitrophenylacetyl (NP)-KLH in alum and ten days after immunization, the frequency and number of NP-specific B cells in the skin-draining LN was determined. Comparing immunized mice with or without concurrent *Hp* infection, the frequency of class-switched IgD⁻ NP-specific B cells was similar between groups suggesting that activation of antigen-specific B cells on a per cell basis was not compromised (Figure 6A and supplemental Figure 2). In contrast, the absolute number of NP-specific B cells in immunized mice infected with *Hp* was significantly decreased compared to uninfected controls (Figure 6B). Concomitantly, serum titers of NP-specific IgG were decreased in helminth-infected mice compared to helminth-naïve animals (Figure 6C). Similar differences in antigen-specific IgG titers were obtained using Pevnar13[®], a clinically relevant pneumococcal vaccine formulation (Figure 6D). To examine whether helminth infection also compromised immunity to heterologous infection at a distinct tissue site, *Hp*-infected or naïve mice were infected with influenza A virus (IAV)²³. Seven days after IAV infection (day 21 post-*Hp* infection), the lung-draining

mediastinal LNs were visibly smaller in helminth-infected mice compared to controls (unpublished observations) and this corresponded with a lower number of total lymphocytes (Figure 6E). In addition, the number of IAV-specific CD8⁺ T effector cells in the mediastinal LNs was decreased in helminth-infected mice and was associated with increased viral burden in lungs compared to control animals (Figure 6F, G). Collectively, these results suggest that helminth infection-induced systemic redistribution of naïve lymphocytes compromises the magnitude of the immune response to heterologous immune challenge and reduced pathogen clearance at distinct barrier sites.

DISCUSSION

Helminth infections almost universally elicit Th2 responses that limit worm burden, promote tissue repair and, in some cases, confer protection from re-infection⁹. However, an excessive Th2 response can be detrimental to the host leading to immunopathology²⁴ and reduced fitness against other infectious agents²⁵⁻²⁷. Our results reveal another previously unknown consequence of enteric helminth infection, namely the systemic and sustained redistribution of the naïve lymphocyte pool away from peripheral LN into the mesLN resulting in compromised immune responses to heterologous peripheral challenge and increased susceptibility to infection. Although helminths including *Hp* produce immunosuppressive factors²⁸, we did not find a change in the frequency of the antigen-specific response in the lymph nodes draining peripheral sites of immunized mice previously infected with *Hp* compared to uninfected controls suggesting a largely unimpeded priming of the heterologous immune response. However, we did observe a significant decrease in the magnitude of T and B effector cell response in three separate antigen-specific models of heterologous challenge. These data argue against direct immunosuppression by helminth-derived factors and instead suggests that an accumulation of naïve lymphocytes in the reactive mesLN compromised the availability of lymphocytes in peripheral lymph nodes and subsequent antigen encounter and activation. Surprisingly, the redistribution and accumulation of naïve lymphocytes in the mesLN of helminth-infected animals was not required to support the effector T cell response. The beneficial function that naïve T lymphocyte accumulation may have on host immunity to helminth infection has yet to be determined. It is tempting to speculate that the increased number of naïve T cells in the mesLN enhances the ability to respond to additional local immune challenges that might be brought about by the compromised barrier integrity as a consequence of helminth-induced tissue damage²⁹. However, as discussed below, the mechanisms driving naïve T cell accumulation may also contribute to the anti-helminth humoral immune response.

Our results indicated that naïve lymphocyte accumulation in the inflamed mesLN required both CD4⁺ T cell activation and LTβR-dependent signals. Harris and colleagues recently demonstrated that LTβ production by B cells acts on CCL19-producing stromal cell populations to reorganize the lymph node structure, induce lymph node hyperplasia and promote *Hp*-specific antibody responses²⁰. Importantly, they found IL-4 to promote LTβ production by B cells in vitro and IL-4 receptor signaling to be critical for mesLN restructuring in vivo. Consistent with these results, we also found expression of IL-4Rα contributes to naïve lymphocyte accumulation and lymph node hyperplasia. Our previous work demonstrated that the dominant source of IL-4 in the reactive mesLN of *Hp*-infected

mice are CD4⁺ T follicular helper (Tfh) cells¹⁵. These studies collectively suggest that, under normal conditions, early IL-4 secretion by Tfh cells promotes LTβ production by follicular B cells that expands LTβR-expressing stromal cells to reorganize the LN architecture. Indeed, we have found IL-4 to be produced by CD4⁺ T cells as early as 5 days post-*Hp* infection, a time point that precedes a detectable germinal center B cell and antibody response³⁰. These results are consistent with another study that also found LTβ production by B cells promotes Th2 responses following *Hp* infection¹⁸. However, we also found B cells to be dispensable for naïve T cell accumulation indicating an additional source of LTβR ligand that compensates for B cell production of LTβ. As our data show that DCs and CD4⁺ T cells express high levels of *Tnfrsf14* mRNA (the gene encoding for LIGHT, an alternate LTβR ligand) compared to B cells and that LIGHT has been previously shown to be important for LN hypertrophy following immunization¹⁹, we suggest that DCs and/or T cells can also directly contribute to enhancing naïve lymphocyte accumulation in reactive lymph nodes. Based on our results and those of others, we speculate that following DC-dependent CD4⁺ T cell priming, T cells produce LTβR ligands or elicit production of these factors by DCs facilitating the accumulation of naïve lymphocytes in the inflamed mesLN. Subsequent IL-4 production by developing Tfh cells stimulates B cell production of LTβ that along with LIGHT promotes stromal cell activation and mobilization. This intercellular IL-4-LTβ signaling network then feeds forward to help position T and B cells to interact in a highly efficient manner to drive the humoral immune response and generate protective antibodies against the intestinal parasite. However, this comes at the cost of compromising immunity to subsequent infection at peripheral sites. Consistent with our studies, deworming individuals prior to BCG vaccination enhances the magnitude of the *M. tuberculosis*-specific T cell response³¹. Our results provide one potential explanation for this clinical benefit and may inform vaccination strategies in regions of the world where helminth infections are endemic.

MATERIAL AND METHODS

Animals

BALB/c, 4get¹², 4get x *Ii4ra* KO, *Tcra* KO, JhD and OVA-TCR transgenic DO11.10 mice all on a BALB/c background and *Ifnar* KO and *Tnfa* KO mice on a C57BL/6 background were bred and kept under specific pathogen-free conditions and used at 8–12 wk of age. All experiments were performed under Institutional Animal Care and Use Committee-approved protocols at the Trudeau Institute and McGill University.

Infections and immunizations

Animals were infected by gavage with 200 third stage larvae of *Heligmosomoides polygyrus* as described¹⁰. In some experiments, adult *Hp* parasites were eliminated by two oral administrations of 100 mg/kg pyrantel pamoate (Columbia Laboratories, Ottawa, Ontario) delivered 2 d apart. For heterologous challenge experiments, some mice were immunized in the footpad with 100µg of NP-KLH (Biosearch technologies) precipitated in alum (Imject 77161, ThermoScientific) or intramuscularly with 0.5µg Prevnar13[®] (Pfizer). Influenza infections were performed intranasally with a sublethal dose (50 PFU) of H1N1 strain A/

Puerto Rico/8/34 in a 25µl volume. Virus was propagated and isolated from Madin-Darby canine kidney (MDCK) cells and titrated with standard plaque assay in MDCK cells²³.

Antibody and LTβR-Ig treatments

At specified time points following *Hp* infection, some mice were i.p. injected with either 100µg anti-CD62L (MEL14) or rat IgG2a isotype control every other day for the indicated period or 150µg LTβR-Ig or control reagent (provided by Biogen) on days 7 and 10 post-*Hp* infection³². Anti-CD4 (GK1.5, 500µg/mouse) or rat IgG2b isotype control was given i.p. one day before infection and CD4⁺ T cell depletion after 2 weeks was still greater than 98% (as determined by staining for TCRβ, CD8α and anti-CD4 (RM4-4)).

T cell transfers

CD4⁺ T cells were FACS sorted from the lymph nodes of Thy1.2⁺ DO11.10 mice and 5×10⁵ cells were transferred i.v. into naive or day 11 *Hp*-infected Thy1.1⁺ recipients. One hour later, the number of donor CD4⁺ T cells present in the mesLN and pooled non-draining inguinal, axillary and brachial skin-draining LN was assessed by flow cytometry.

Flow cytometry

Single cell suspensions were prepared from the mesenteric or non-draining lymph nodes, stained and analyzed as described¹⁰. The following mAbs were used for flow cytometry; clone designations are given in parenthesis: CD4 (RM4-5, RM4-4), CD8α (53-6.7), CD19 (1D3), B220 (RA3-6B2), CD11c (N418), MHCII (M5/114.15.2), CD62L (MEL-14), CD44 (IM7), IgD (11-26c), DO11.10 TCR (KJ1-26), Thy1.1 (OX7), Thy1.2 (53-2.1) (BD biosciences, eBiosciences or Biolegend). NP was conjugated to APC as reported³³ and used in standard antibody staining procedures for antigen-specific B cell detection. Influenza-specific CD8⁺ T cells were identified with NP (ASNENMETM)-loaded H-2D^b tetramers conjugated to APC (1:600 dilution; National Institutes of Health Tetramer Core Facility, Emory University Vaccine Center). Propidium iodide or fixable viability dye (eBiosciences) was used to eliminate dead cells from analysis. Staining for intracellular active Caspase-3 (C92-605) was performed using Cytofix/Cytoperm reagents as suggested by the manufacturer (BD Biosciences). Samples were acquired on a FACS Canto II or LSR Fortessa (BD Biosciences) and analyzed with FlowJo software (Tree Star, Inc.).

ELISA

Serotype 3 *Streptococcus pneumoniae* polysaccharide-specific IgG was detected in serum 4-5 weeks following i.m. challenge by polysaccharide-specific ELISA. Briefly, 96 well plates were coated with purified polysaccharide (ATSS) overnight, washed and serum dilutions were applied. HRP anti-mouse IgG detecting antibody (Southern Biotech) was applied, developed with ABTS buffer and read on a Molecular Devices SPECTRAMax Plus 384 at 405nm. NP-specific IgG was detected in serum by heteroclitic NIP (4-hydroxy-5-iodo-3-nitrophenyl)-specific ELISA as described³³. Protocol was identical to polysaccharide ELISA except plates were coated with NIP(11)-OVAL and an IgG anti-NP standard (clone PeVch 1/λ1, BioXcell) was used.

qRT-PCR

mesLN cells were sorted into the populations described in Figure 4 using a FACS Aria III prior to RNA extraction. mRNA was extracted using Qiagen RNeasy Micro Kit and cDNA samples were prepared as previously described¹⁵. Custom primer sequences were generated using Primer3 software for the following genes: *Lta*, Fwd:

CAGCAAGCAGAACTCACTGC, Rev: CACTGAGGAGAGGCACATGG; *Ltb*, Fwd:

ACCTCATAGGCGCTTGGATG, Rev: ACGCTTCTTCTTGGCTCGC; *Tnfsf14*, Fwd:

GCATGGAGAGTGTGGTACAGC and Rev: TGTCTCCAAGACGTTGATGC and *Hprt*,

Fwd: AGGACCTCTCGAAGTGTGG and Rev: AACTTGCCTCATCTTAGGC.

Quantitative real-time RT-PCR was performed by sybr green detection using the Biorad CFX96TM Real-Time System and software. Fold expression was calculated using the $2^{-\Delta\Delta CT}$ method and *Hprt* as a reference gene.

Confocal fluorescence microscopy

Frozen mesLN cut into 7 μm sections were embedded in optimum cutting temperature compound and labeled with anti-B220 (RA3-6B2), anti-GL7 (GL7) and anti-CD4 (RM4-5) from BD biosciences. Fluorescent images were obtained with a TCS SP5 confocal microscope and 'stitched' high-resolution whole LN confocal images were obtained using LAS AF 2.2.1 software (Leica).

Statistical analysis

GraphPad Prism (version 5) was used for statistical analysis. Data sets were compared by unpaired, two-tailed Student's or Mann-Whitney *t* test with the exception of Figure 1C and 4G in which a one-way ANOVA was used followed by a Tukey's post-hoc analysis. Data are represented as mean \pm SEM if not indicated otherwise. ns, not significant; *, $p < 0.05$; **, $p < 0.01$; ***, $p < 0.001$.

Supplementary Material

Refer to Web version on PubMed Central for supplementary material.

Acknowledgments

We thank Dr. Ghislaine Fontés for her technical assistance in the completion of this work. This research was supported by funds from Trudeau Institute, the National Institutes of Health grant AI076479 (M.M.), McGill University Faculty of Medicine (I.L.K.) and the Canadian Institutes of Health Research grant 130579. I.L.K. also holds a Canada Research Chair Award.

References

1. Takada K, Jameson SC. Naive T cell homeostasis: from awareness of space to a sense of place. *Nature reviews Immunology*. 2009; 9:823–832.
2. Link A, et al. Fibroblastic reticular cells in lymph nodes regulate the homeostasis of naive T cells. *Nature immunology*. 2007; 8:1255–1265. [PubMed: 17893676]
3. Hataye J, Moon JJ, Khoruts A, Reilly C, Jenkins MK. Naive and memory CD4+ T cell survival controlled by clonal abundance. *Science*. 2006; 312:114–116. [PubMed: 16513943]
4. Angeli V, et al. B cell-driven lymphangiogenesis in inflamed lymph nodes enhances dendritic cell mobilization. *Immunity*. 2006; 24:203–215. [PubMed: 16473832]

5. Yang CY, et al. Trapping of naive lymphocytes triggers rapid growth and remodeling of the fibroblast network in reactive murine lymph nodes. *Proceedings of the National Academy of Sciences of the United States of America*. 2014; 111:E109–118. [PubMed: 24367096]
6. Soderberg KA, et al. Innate control of adaptive immunity via remodeling of lymph node feed arteriole. *Proceedings of the National Academy of Sciences of the United States of America*. 2005; 102:16315–16320. [PubMed: 16260739]
7. Webster B, et al. Regulation of lymph node vascular growth by dendritic cells. *The Journal of experimental medicine*. 2006; 203:1903–1913. [PubMed: 16831898]
8. Pham TH, Okada T, Matloubian M, Lo CG, Cyster JG. S1P1 receptor signaling overrides retention mediated by G alpha i-coupled receptors to promote T cell egress. *Immunity*. 2008; 28:122–133. [PubMed: 18164221]
9. Anthony RM, Rutitzky LI, Urban JF Jr, Stadecker MJ, Gause WC. Protective immune mechanisms in helminth infection. *Nature reviews Immunology*. 2007; 7:975–987.
10. Mohrs K, Wakil AE, Killeen N, Locksley RM, Mohrs M. A two-step process for cytokine production revealed by IL-4 dual-reporter mice. *Immunity*. 2005; 23:419–429. [PubMed: 16226507]
11. Urban JF Jr, Katona IM, Paul WE, Finkelman FD. Interleukin 4 is important in protective immunity to a gastrointestinal nematode infection in mice. *Proceedings of the National Academy of Sciences of the United States of America*. 1991; 88:5513–5517. [PubMed: 2062833]
12. Mohrs M, Shinkai K, Mohrs K, Locksley RM. Analysis of type 2 immunity in vivo with a bicistronic IL-4 reporter. *Immunity*. 2001; 15:303–311. [PubMed: 11520464]
13. Perona-Wright G, Mohrs K, Mayer KD, Mohrs M. Differential regulation of IL-4Ralpha expression by antigen versus cytokine stimulation characterizes Th2 progression in vivo. *Journal of immunology*. 2010; 184:615–623.
14. Mempel TR, Henrickson SE, Von Andrian UH. T-cell priming by dendritic cells in lymph nodes occurs in three distinct phases. *Nature*. 2004; 427:154–159. [PubMed: 14712275]
15. King IL, Mohrs M. IL-4-producing CD4+ T cells in reactive lymph nodes during helminth infection are T follicular helper cells. *The Journal of experimental medicine*. 2009; 206:1001–1007. [PubMed: 19380638]
16. McLachlan JB, et al. Mast cell-derived tumor necrosis factor induces hypertrophy of draining lymph nodes during infection. *Nature immunology*. 2003; 4:1199–1205. [PubMed: 14595438]
17. Shioh LR, et al. CD69 acts downstream of interferon-alpha/beta to inhibit S1P1 and lymphocyte egress from lymphoid organs. *Nature*. 2006; 440:540–544. [PubMed: 16525420]
18. Leon B, et al. Regulation of T(H)2 development by CXCR5+ dendritic cells and lymphotoxin-expressing B cells. *Nature immunology*. 2012; 13:681–690. [PubMed: 22634865]
19. Zhu M, Yang Y, Wang Y, Wang Z, Fu YX. LIGHT regulates inflamed draining lymph node hypertrophy. *Journal of immunology*. 2011; 186:7156–7163.
20. Dubey LK, et al. Lymphotoxin-Dependent B Cell-FRC Crosstalk Promotes De Novo Follicle Formation and Antibody Production following Intestinal Helminth Infection. *Cell Rep*. 2016
21. Moussion C, Girard JP. Dendritic cells control lymphocyte entry to lymph nodes through high endothelial venules. *Nature*. 2011; 479:542–546. [PubMed: 22080953]
22. Moon JJ, et al. Naive CD4(+) T cell frequency varies for different epitopes and predicts repertoire diversity and response magnitude. *Immunity*. 2007; 27:203–213. [PubMed: 17707129]
23. Coulombe F, et al. Targeted prostaglandin E2 inhibition enhances antiviral immunity through induction of type I interferon and apoptosis in macrophages. *Immunity*. 2014; 40:554–568. [PubMed: 24726877]
24. Pearce EJ, MacDonald AS. The immunobiology of schistosomiasis. *Nature reviews Immunology*. 2002; 2:499–511.
25. Osborne LC, et al. Coinfection. Virus-helminth coinfection reveals a microbiota-independent mechanism of immunomodulation. *Science*. 2014; 345:578–582. [PubMed: 25082704]
26. Potian JA, et al. Preexisting helminth infection induces inhibition of innate pulmonary anti-tuberculosis defense by engaging the IL-4 receptor pathway. *The Journal of experimental medicine*. 2011; 208:1863–1874. [PubMed: 21825018]

27. Salgame P, Yap GS, Gause WC. Effect of helminth-induced immunity on infections with microbial pathogens. *Nature immunology*. 2013; 14:1118–1126. [PubMed: 24145791]
28. Grainger JR, et al. Helminth secretions induce de novo T cell Foxp3 expression and regulatory function through the TGF-beta pathway. *The Journal of experimental medicine*. 2010; 207:2331–2341. [PubMed: 20876311]
29. Su CW, et al. Duodenal helminth infection alters barrier function of the colonic epithelium via adaptive immune activation. *Infection and immunity*. 2011; 79:2285–2294. [PubMed: 21444669]
30. Meli AP, et al. The Integrin LFA-1 Controls T Follicular Helper Cell Generation and Maintenance. *Immunity*. 2016; 45:831–846. [PubMed: 27760339]
31. Elias D, et al. Effect of deworming on human T cell responses to mycobacterial antigens in helminth-exposed individuals before and after bacille Calmette-Guerin (BCG) vaccination. *Clinical and experimental immunology*. 2001; 123:219–225. [PubMed: 11207651]
32. Wang Y, et al. Lymphotoxin beta receptor signaling in intestinal epithelial cells orchestrates innate immune responses against mucosal bacterial infection. *Immunity*. 2010; 32:403–413. [PubMed: 20226692]
33. King IL, et al. Invariant natural killer T cells direct B cell responses to cognate lipid antigen in an IL-21-dependent manner. *Nature immunology*. 2012; 13:44–50.

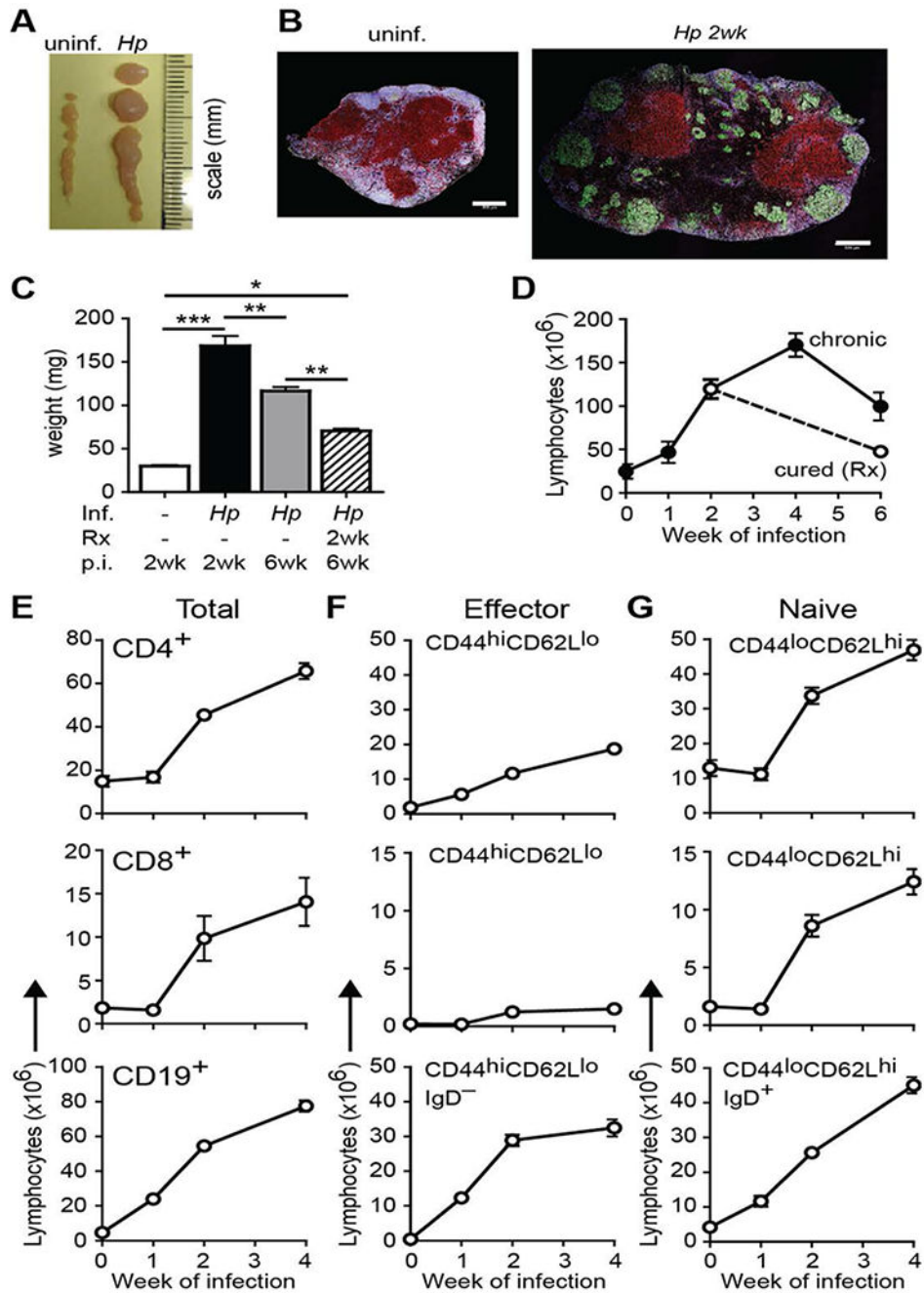


Figure 1. Naïve lymphocytes accumulate in the Th2 reactive mesLN following intestinal helminth infection

BALB/c mice were infected with *Hp* or remained naïve and the mesLN were collected at the indicated time points. (A) Representative image of mesLN from naïve and 2 wk *Hp*-infected animals. (B) Confocal immunofluorescent images of uninfected and 2 wk *Hp* infected mesLN. B220, white; CD4, red; GL7, green. Bar, 500 μ m. (C) MesLN weight from naïve and *Hp* infected animals. Some mice received anti-helminthics at 2 weeks post-*Hp* infection; p.i., post-infection. (D) Number of total or (E) CD4⁺, CD8⁺, and CD19⁺ lymphocytes in the mesLN at the indicated times after infection. (F) Number of effector and (G) naïve

phenotype CD4⁺, CD8⁺ and CD19⁺ lymphocytes at the indicated time points after infection. Each data point shows the mean of 4-5 individual mice and error bars indicate the SEM. Data are representative of at least three independent experiments. *p < .05, **p < .01, ***p < .001.

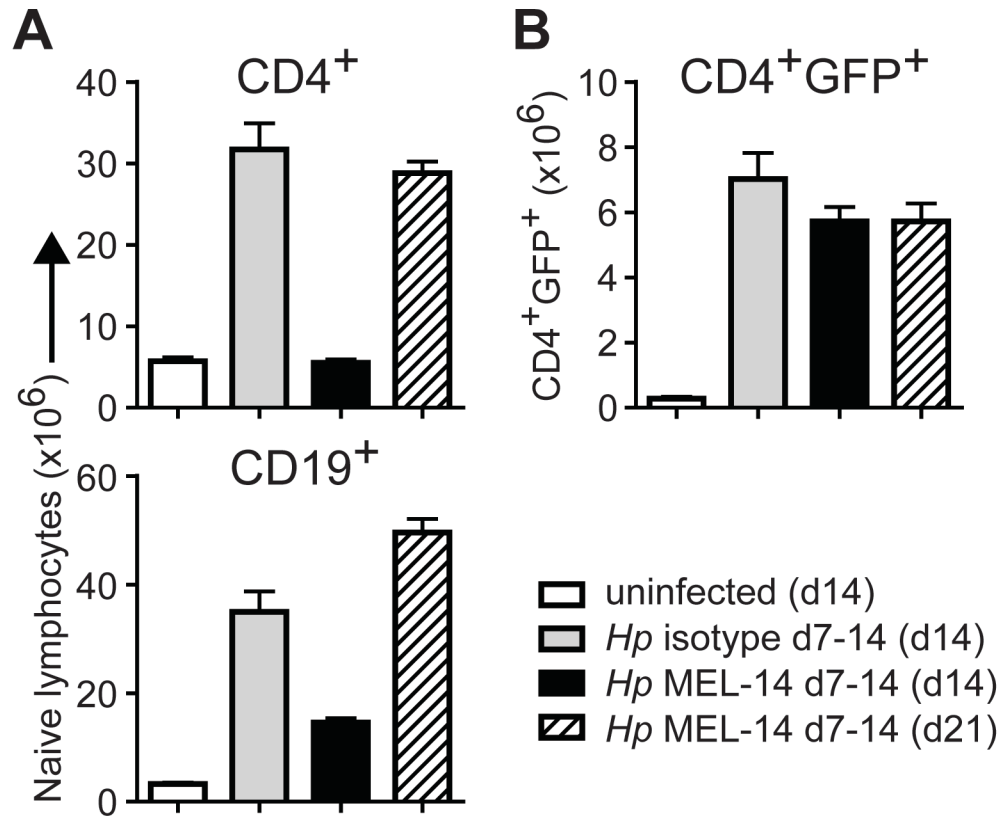


Figure 2. Delayed naive lymphocyte accumulation is dispensable for IL-4⁺ effector CD4 T cell differentiation

BALB/c 4get mice were infected with *Hp* or remained uninfected and were treated every other day with anti-CD62L (MEL-14) or rIgG2a isotype control during the indicated period. MesLN were analyzed on day 14 or 21 post-infection as specified in parentheses. (A) Number of naïve phenotype CD4⁺ and CD19⁺ lymphocytes. (B) Number of GFP⁺IL-4⁺ effector CD4 T cells. Each data point shows the mean of 4-5 individual mice and error bars indicate the SEM. Data are representative of two independent experiments.

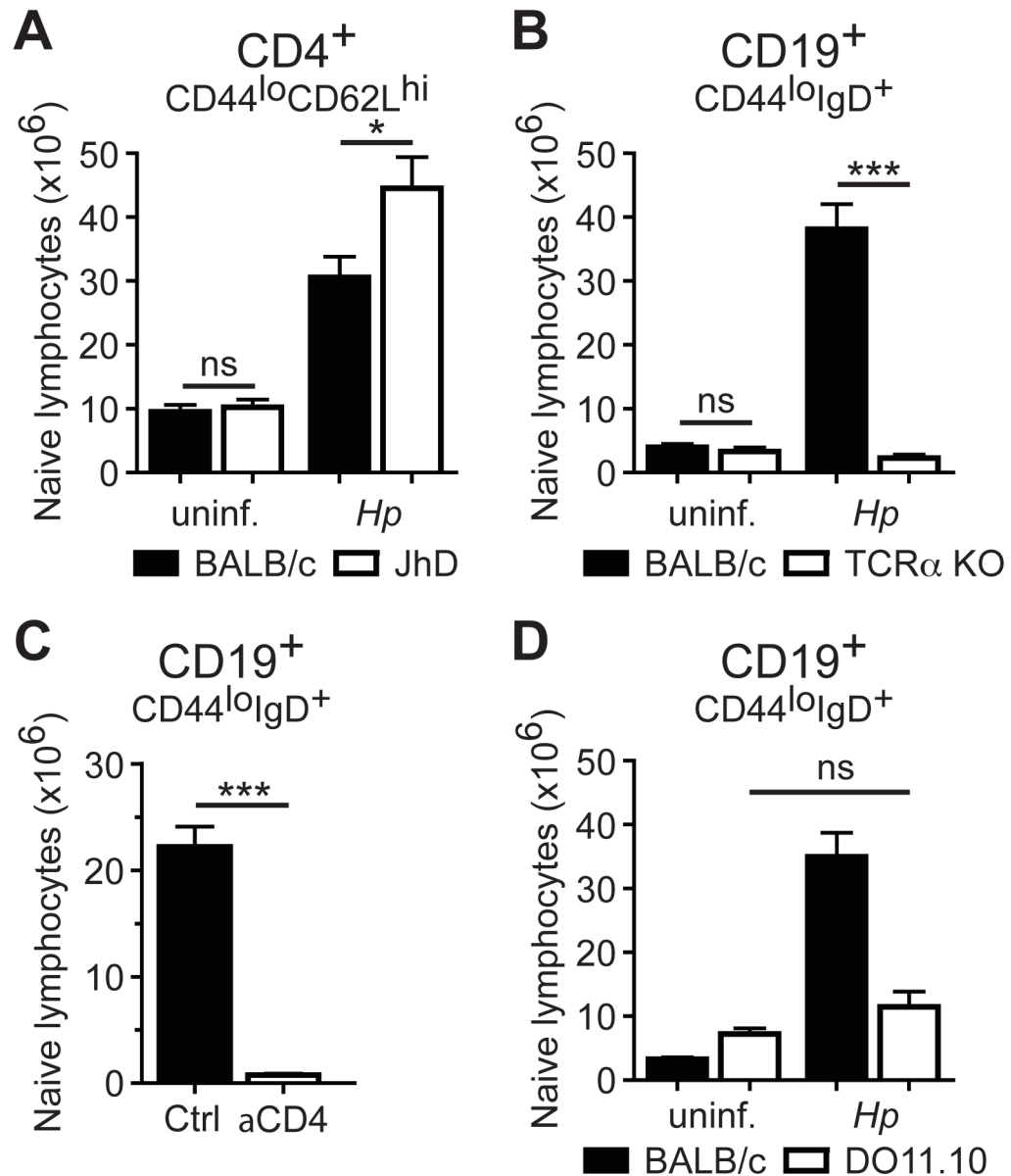


Figure 3. CD4⁺ T cell activation is required for naïve B lymphocyte accumulation

(A) B cell deficient JhD mice and BALB/c WT controls were infected with *Hp* or remained uninfected and the number of naïve phenotype CD4⁺ T cells in the mesLN was analyzed 2 wk later. (B) T cell deficient TCR α KO mice and BALB/c WT controls were infected with *Hp* or remained naïve and the number of naïve phenotype CD19⁺ B cells in the mesLN was analyzed 2 wk later. (C) BALB/c mice were treated with anti-CD4 or rIgG2b isotype control and infected with *Hp* one day later. The number of naïve phenotype CD19⁺ B cells in the mesLN was determined at 2 wk post-infection. (D) DO11.10 TCR transgenic mice and BALB/c WT controls were infected with *Hp* and the number of naïve phenotype CD19⁺ B cells in the mesLN was determined at 2 wk post-infection. Each data point shows the mean of 3-5 individual mice and error bars indicate the SEM. Data are representative of at least two independent experiments. ns, not significant; *p < .05, ***p < .001.

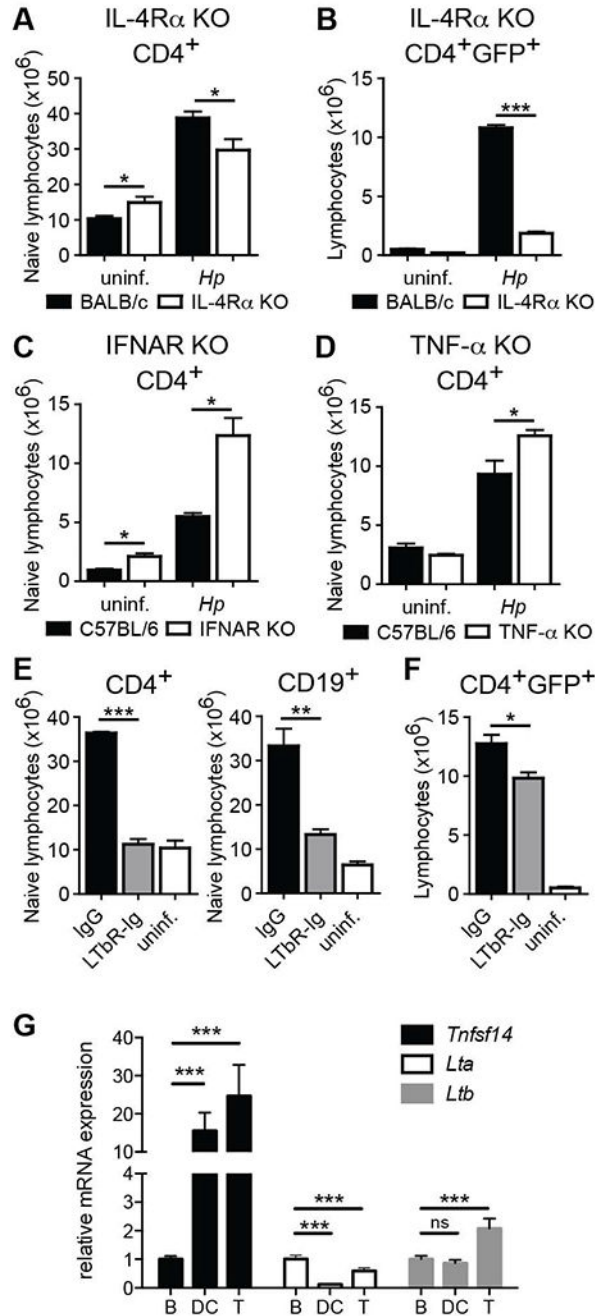


Figure 4. Lymphotoxin- β receptor signaling is required for naïve lymphocyte accumulation (A, B) IL-4R α deficient and WT BALB/c 4get mice were infected with *Hp* or remained naïve and the number of naïve (A) or IL-4/GFP⁺ effector (B) CD4⁺ T cells in the mesLN was analyzed at 2 wk post-infection. IFNAR KO mice (C) or TNF- α KO mice (D) as well as C57BL/6 WT controls were infected with *Hp* or remained naïve. The number of naïve phenotype CD4⁺ T cells in the mesLN was determined 2 wk later. (E, F) BALB/c 4get mice were infected with *Hp* and LT β R-Ig or control IgG was administered i.p. on days 7 and 10 after infection. The number of naïve CD4⁺ T and CD19⁺ B cells (E) or effector phenotype

CD4⁺ T cells (F) in the mesLN was analyzed at 2 wk post-infection. (G) B220⁺CD4⁻ B cells, CD11c⁺MHCII⁺ and CD4⁺B220⁻ T cells were sorted from the mesLN of 2 week *Hp*-infected mice and mRNA from each population was assessed by qRT-PCR for the indicated transcripts. Each group shows the mean of 8 individual mice and error bars indicate the SEM. Data are representative of at least two independent experiments. ns, not significant; *p < .05, **p < .01 ***p < .001.

Author Manuscript

Author Manuscript

Author Manuscript

Author Manuscript

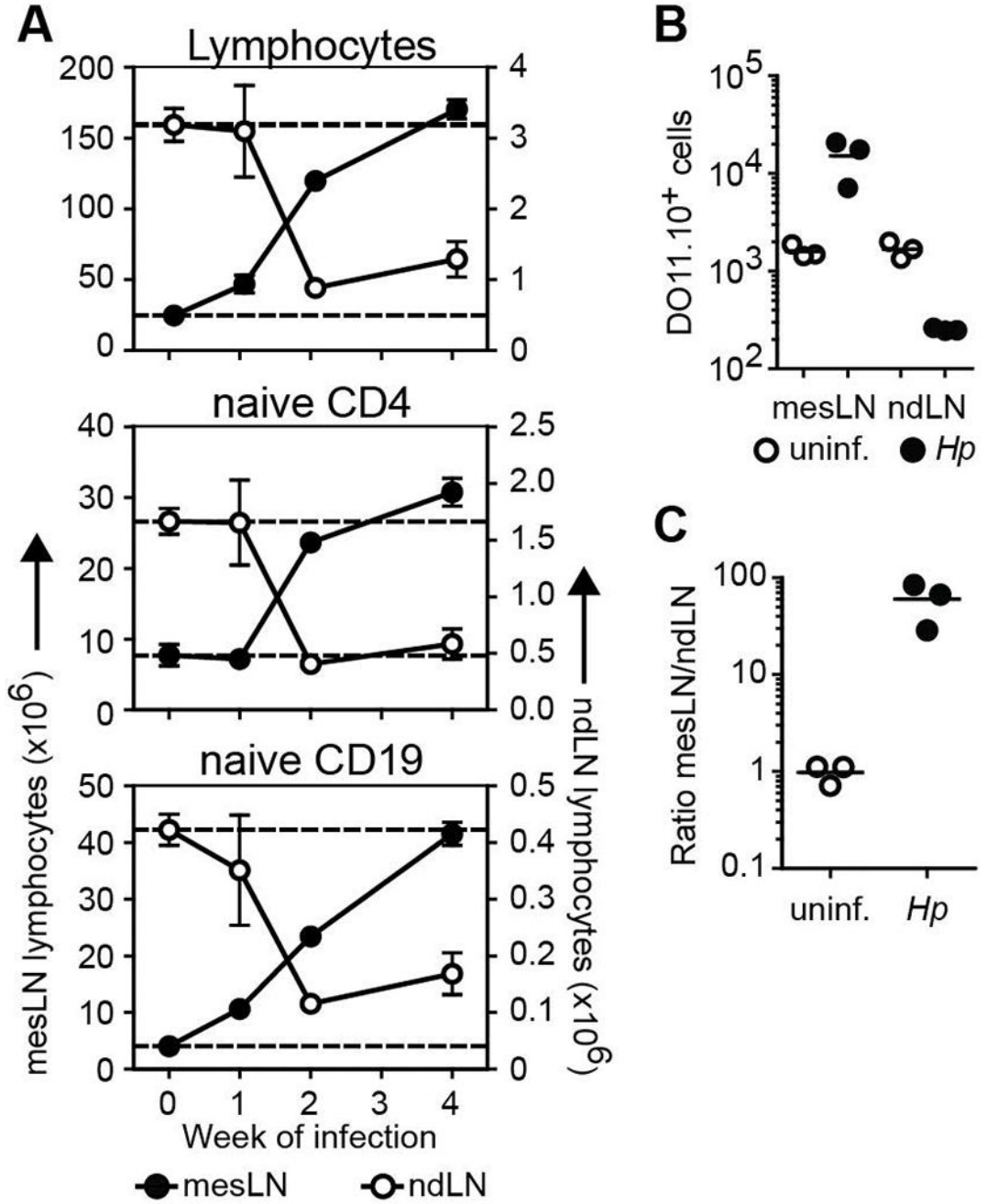


Figure 5. Intestinal helminth infection results in the systemic and sustained redistribution of the naive lymphocyte pool

(A) BALB/c or 4get BALB/c mice were infected with *Hp* and the number of total lymphocytes and naive phenotype CD4⁺ T and CD19⁺ B cells in the mesLN (left Y axis) and the pooled non-draining inguinal, axillary and brachial LN (ndLN) (right Y axis) were determined at the indicated time points. Each data point shows the mean of 3-5 individual mice and error bars indicate the SEM. Data are representative of at least two independent experiments. (B) OVA-specific CD4⁺ T cells from Thy1.2⁺ DO11.10 mice were transferred into uninfected or day 11 *Hp* infected Thy1.1⁺ congenic mice. The number of

Thy1.2⁺KJ1-26⁺ donor CD4⁺ T cells in the mesLN or the pooled non-draining inguinal, axillary and brachial LN (ndLN) was determined one hour later by flow cytometry. (C) The relative recruitment of DO11.10 donor cells into the mesLN relative to the ndLN was calculated based on the total numbers determined in B. Scatter plots in B and C show data from individual mice. Data are representative of two independent experiments with 3 mice per group.

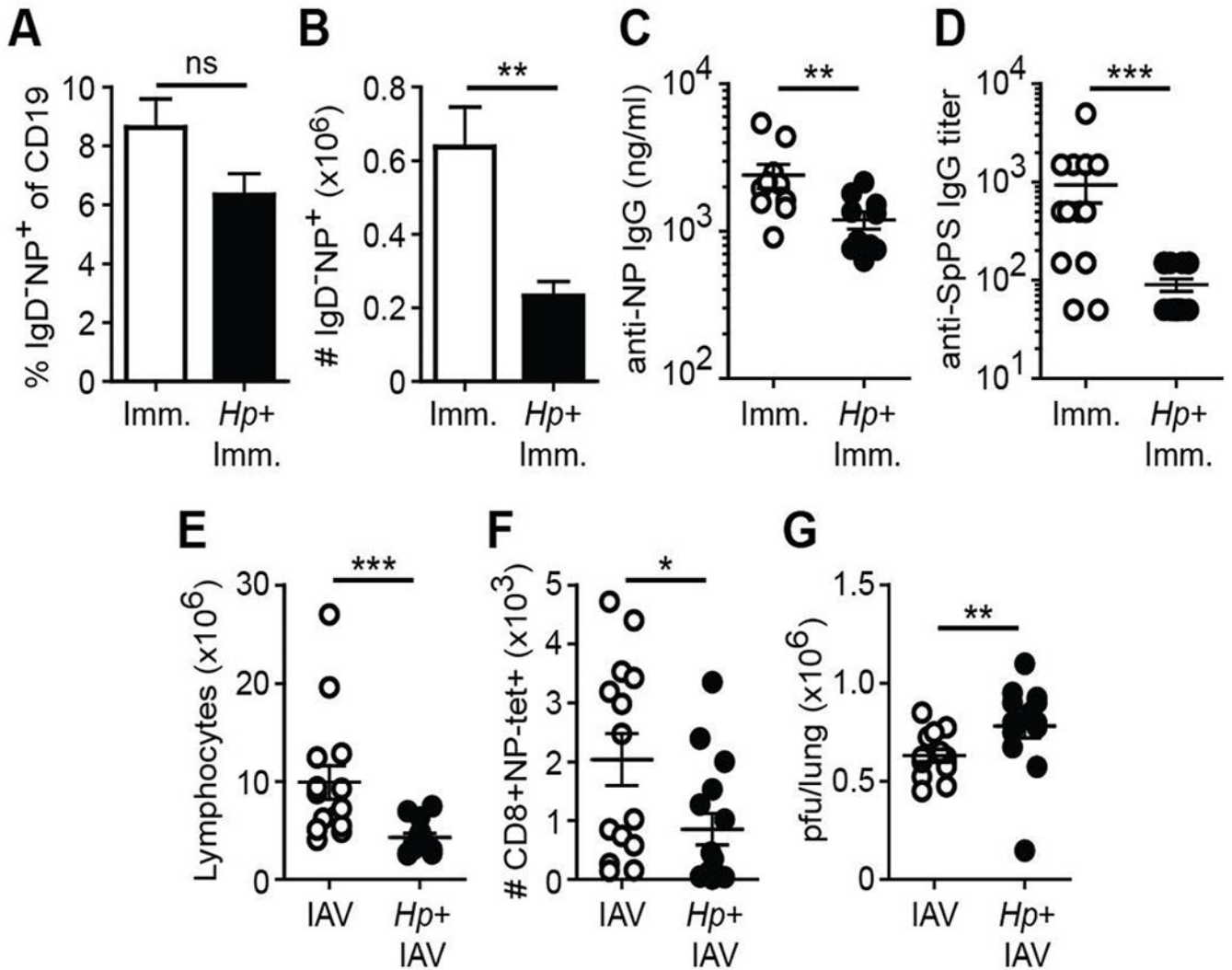


Figure 6. Intestinal helminth compromises immunity to heterologous challenge at peripheral sites

C57BL/6 mice were infected with *Hp* or remained naïve. Two weeks later the animals were heterologously challenged. (A-C) One week after footpad immunization with NP-KLH in alum, the frequency (A) and number (B) of IgD⁻ isotype switched NP-specific B cells in the draining popliteal LNs were determined by flow cytometry. (C) Serum anti-NP IgG titers at day 21 after NP-KLH immunization. (D) *Hp*-infected or naïve mice were immunized i.m. with the anti-pneumococcal vaccine formulation Prevnar13[®] and anti-*S. pneumoniae* polysaccharide IgG titers were determined 4-5 weeks later. (E, F) Number of total (E) or influenza (IAV)-specific CD8⁺ effector T lymphocytes (F) from the mediastinal LN of *Hp*-infected or helminth-naïve animals 7 days after i.n. infection with 50 pfu IAV. (G) Pulmonary viral load (pfu) was determined at day 7 post-IAV infection. Data shown is pooled from two independent experiments containing a total of 14-15 mice/group. Error bars indicate the SEM. ns, not significant; **p* < .05, ***p* < .01 ****p* < .001.